INTERFERENCE CANCELLATION IN TWO-CHANNEL NUCLEAR QUADRUPOLE RESONANCE MEASUREMENTS

Tommaso Piatti[*]*, Shiwen Lei*[*]*, Jamie Barras*[†]*, and Andreas Jakobsson*[*]

[*]Centre for Mathematical Sciences, Lund University, Sweden
[†]Department of Informatics, King's College London, UK
emails: {tommaso, shiwen, aj}@maths.lth.se, jamie.barras@kcl.ac.uk

ABSTRACT

Given its high specificity, the use of nuclear quadrupole resonance (NQR) spectroscopy allows for a reliable identification and quantification of substances containing quadrupolar nuclei, such as the ^{14}N nucleus prevalent in many explosives, medicines, and narcotics. Regrettably, the measured signals are typically weak and suffers from interference signals often being several orders of magnitude stronger than the signal of interest. In this work, we propose a two-channel setup allowing for interference cancellation in applications such as demining. The proposed techniques forms an estimate of the interference using the secondary channel, and then removes it from the primary channel. The improved performance of the resulting detector is illustrated using real measurements of $NaNO_2$.

Index Terms— Interference cancellation, radio frequency spectroscopy, multi-channel data

1. INTRODUCTION

Nuclear quadrupole resonance (NQR) is a radio frequency (RF) spectroscopic technique which can be used to detect the presence of quadrupolar nuclei, a requirement fulfilled by roughly 50% of the elements in the periodic table (see, e.g., [1]). The technique is similar to both nuclear magnetic resonance (NMR) and magnetic resonance imaging (MRI), but unlike these, NQR does not require a large static magnetic field to split the energy levels of the nucleus, allowing for both relatively cheap and portable sensor equipment. The acquired NQR signals are highly specific, allowing for an unequivocal identification of a large range of solid-state explosives and narcotics, with obvious applications in the detection of explosives in landmines and unexploded ordnance, as well as quantification of the content of many forms of medicines, for instance allowing for the non-invasive detection of counterfeit or substandard medicines [2–9]. Regrettably, the acquired signals are often weak and suffers from the presence of strong RF interference (RFI), such as the spurious signals resulting from piezoelectric- and magnetoacoustic responses or from the radio transmissions present in RF band of interest. Such RFI may often be several magnitudes stronger than the signal-of-interest (SOI), necessitating efficient interference cancellation to allow for a practically useable system. During recent years, notable efforts have been made to improve experimental setups and to develop detection algorithms allowing both for uncertainties in the model assumptions and in the temperature of the observed substance, and for RFI cancellation using secondary data [10–17]. Reliable RFI cancellation is difficult both due to the magnitude of the RFI and by its highly non-stationary nature. Furthermore, to allow for a reasonable signal-to-noise ratio (SNR), it is often necessary to use probes with a high Q factor, resulting in the excitation of only a narrow band of frequencies, causing the RFI to be close or even coinciding with the SOI frequencies. Efforts made to cancel the interference using secondary data, such as those in [18–21], although efficient, suffers from the rapidly changing nature of the RFI, especially in the high-Q case when RFI components frequently occur close to, or even coincides, with the SOI, while still varying too rapidly to allow for the use of secondary data acquired while the spins relaxes back to their original state. In this work, we develop a two-channel NQR setup specifically tailored for this case. Multi-channel NQR techniques have been proposed earlier (see, e.g., [12, 22]), although these techniques assume that the RFI components remain reasonably stationary over the acquisition. Here, we instead introduce the use of the second channel as a way of estimating the RFI impinging simultaneously on the primary sensor, which will measure both the SOI and the RFI. Generally, the two sensors will have different gains, and although impinging simultaneously on the both channels, the RFI will be somewhat different in the two channels. The proposed RFI cancellation algorithm tracks the time-varying gain between the sensors and subtracts the estimated RFI component from the primary channel, thereby allowing for the presence of rapidly varying RFI that may be close, or even coincide, with the SOI. The improved performance of the resulting detector is illustrated using measurements of $NaNO_2$.

This work was supported in part by the Swedish Research Council and Carl Trygger's foundation.

2. SIGNAL MODEL

For substances having a long spin-lattice relaxation time, such as, e.g., the explosive TNT, measurements are generally acquired using so-called pulse spin locking (PSL) sequences, formed by a train of excitation pulses which aims at refocusing the magnetization. The resulting signal constitutes a train of decaying echoes, each being well modelled as a sum of decaying sinusoids, with frequencies depending on the temperature of the observed substance [14, 23]. For notational simplicity, we will here denote the resulting $N \times 1$ dimensional SOI vector $\mathbf{s}(t;\theta)$, with t denoting the echo number, and θ the unknown parameters detailing the SOI. These typically include the temperature of the observed substance, the decay rates of the echoes, as well as the echo train, as well as further parameters not relevant for the present discussion [23].

Generally, the sensors' gain will be different, as well as vary slowly over time due to the sensors heating up during the measurements. In order to allow for this, the system is set up to measure two sets of data for each channel; initially, both channels measure the background, prior to the actual sensing, thereby allowing for measurements useful to estimate the gain difference between the sensors. Then, when exposed to the substance of interest, the primary sensor will record the contribution of the SOI, whereas the secondary sensor, due to the spatial offset to the substance, will only measure the noise and interference. The signal measured on the primary channel, $\mathbf{y}_p(t)$, may thus be modelled as

$$\mathbf{y}_p(t) = \mathbf{s}(t;\theta) + \mathbf{r}_p(t) + \mathbf{e}_p(t) \tag{1}$$

where $\mathbf{r}_p(t)$ denotes a sum of rapidly time-varying narrowband RFI components, and $\mathbf{e}_p(t)$ an unstructured thermal (Johnson) noise, often assumed to be white circularly symmetric Gaussian distributed (see also [13, 14]). Similarly, the signal measured on the secondary channel, $\mathbf{y}_s(t)$, may be modelled as

$$\mathbf{y}_s(t) = \mathbf{r}_s(t) + \mathbf{e}_s(t) \tag{2}$$

where $\mathbf{r}_s(t)$ denotes the RFI as observed from the second sensor, which typically shares some of its spectral support with $\mathbf{r}_p(t)$, and $\mathbf{e}_s(t)$ the sensor noise. The corresponding measurements made before being exposed to the substance of interest, the so-called pre-measurements, termed $\mathbf{z}_s(t)$ and $\mathbf{z}_p(t)$, have a similar composition, although the primary channel in this case lacks the contribution of the SOI.

3. INTERFERENCE CANCELLATION

Due to the rapidly varying nature of the RFI, one should not use the overall power of the sensors in order to estimate the gain between the sensors, as this will be rapidly varying with frequency for the two sensors. Instead, we focus on the most dominant RFI component present, as at least this is likely to be present in both channels. In order to determine the relative gain between the sensors, we thus proceed to determine the strongest spectral component in the excitation band of either of the two channels; this may be done in various ways, but is here simply done using the maximum of the periodogram within the band. We then estimate the corresponding spectral amplitude of the other channel at the same frequency as this dominant component using least squares (LS). Terming the resulting magnitude estimate of the dominant spectral component $\alpha_p(t)$ and $\alpha_s(t)$ for the primary and secondary sensor at data block t, respectively, the relative gain ratio between the sensors are then estimated for each data block as

$$\rho(t) = \frac{\alpha_p(t)}{\alpha_s(t)} \tag{3}$$

for all measured data blocks in the pre-measurements. Figure 1 shows the time-varying gain of a typical experimental setup, clearly illustrating both the rapidly varying nature of the RFI, and the instability of the resulting gain estimate. As $\rho(t)$ will typically vary noticeably, as illustrated in Figure 1, we proceed to compute the overall gain as as the median of the available $\rho(t)$ estimates, terming the result gain ratio $\hat{\rho}$.

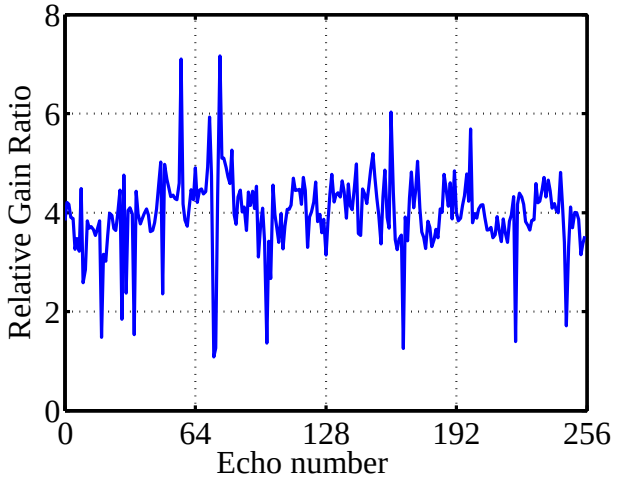

Fig. 1. Relative gain between the channels for the dominant component of the pre-measurements.

Proceeding, we then strive to remove the dominant RFI components from the primary channel using the RFI detected on the secondary channel. For each data block, this is done by estimating the most dominant component in $\mathbf{y}_s(t)$; we term the frequency and amplitude of this component $f_s(t)$ and $\beta_s(t)$, respectively. As the phase of the RFI at the different channels seem to vary significantly and seemingly without any pattern, we proceed to estimate the phase of the corresponding spectral amplitude in the primary channel, at the frequency $f_s(t)$, here termed $\hat{\phi}_p(t)$, using LS, and then form

$$q_p(t) = \hat{\rho}\,|\beta_s(t)|\,e^{2\pi i f_s(t) - 2\pi i \hat{\phi}_p(t)} \tag{4}$$

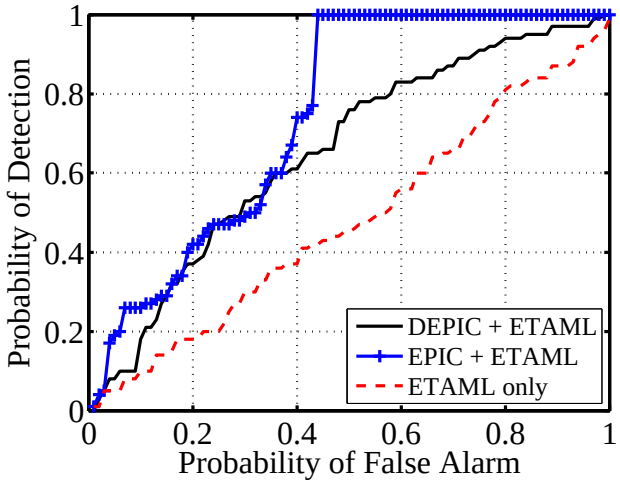

Fig. 2. The ROC for the discussed interference cancellation algorithms, when used in combination with ETAML, for (simplistic) simulation data.

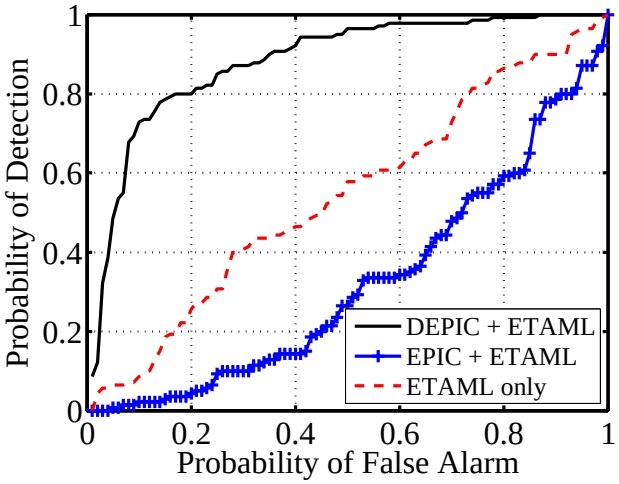

Fig. 3. The ROC for the discussed interference cancellation algorithms, when used in combination with ETAML, for measured $NaNO_2$ data.

which is thus an estimate of the RFI contribution at frequency $f_s(t)$ in the primary channel, scaled with the relative gain ratio to be of the appropriate scale, and aligned to have the same phase as the RFI component in the primary channel. To ensure that one does not subtract more power than is present in the primary channel at this frequency, let

$$\tilde{q}_p(t) = \min\Big\{ |q_p(t)|, |\beta_p(t)| \Big\} \tag{5}$$

where $\beta_p(t)$ denotes the LS estimate of the (complex-valued) amplitude of the primary data at frequency $f_s(t)$, such that

$$\beta_p(t) = \left(\mathbf{a}_f^* \mathbf{a}_f\right)^{-1} \mathbf{a}_f^* \mathbf{y}_p(t) \tag{6}$$

with $(\cdot)^*$ denoting the conjugate transpose, and

$$\mathbf{a}_f = \left[\begin{array}{cccc} 1 & e^{2\pi i f_s(t)} & \ldots & e^{2\pi i f_s(t)(N-1)} \end{array} \right]^T \tag{7}$$

This ensures that $\tilde{q}_p(t)$ does not contain more power than what is present in the primary channel at frequency $f_s(t)$. To further allow for the unreliable gain estimate, and take the estimation errors of the phase and amplitudes into account, we proceed to form the cleaned version of the primary data, $\mathbf{y}_p^{(1)}(t)$, as

$$\mathbf{y}_p^{(1)}(t) = \mathbf{y}_p(t) - \nu \tilde{q}_p(t) \mathbf{a}_f \tag{8}$$

where $0 < \nu \leq 1$ is a user parameter determining how reliable one deems the estimated RFI component. In order to ensure that one does not fully remove a possible SOI contribution, ν is typically selected somewhat lower than unity; in this work, we have from several experimental studies selected $\nu = 0.95$ as being a suitable value. If further RFI components are deemed present in both the primary and secondary channels, one may then proceed to remove further components by repeating the above procedure, forming $\mathbf{y}_p^{(2)}(t)$ by extracting the second largest RFI component from $\mathbf{y}_p^{(1)}(t)$, and so forth. However, our experimental studies indicate that it is difficult to appropriately select the number of such components reliably, given their rapidly time-varying nature, and we have here, for now, thus restricted the interference cancellation to remove only the most dominant RFI component. We will in our continued work strive to determine a suitable estimator for the appropriate RFI model order.

4. NUMERICAL RESULTS

We proceed to examine the proposed RFI cancellation scheme when applied to both simulated and measured NQR data. For the simulation setup, we generate an NQR signal mimicking the echo train signal resulting from an PSL excitation of $NaNO_2$, adding white circular Gaussian noise to model the thermal noise (the precise details of the signal are not relevant to the discussion here and are therefore omitted in the interest of brevity; the reader is referred to [14] for further details on the used model). To simulate a simplistic *stationary* RFI component, we then add a sinusoid with random amplitude coinciding with the frequency of the NQR response from $NaNO_2$. To allow for the difference in gain, we allow the amplitudes to differ somewhat between the channels. The real measurements were formed using PSL sequences on a sample of $NaNO_2$, with both the pre- and actual measurements containing 256 data blocks, each being $N = 128$ samples long[1]. The experiment was repeated 140 times to allow for compu-

[1]Here, each of these measurements were constructed using the phase-cycling of eight measurements, to allow for an efficient cancellation of the ring-down effects; see [24] for a further discussion on this aspect.

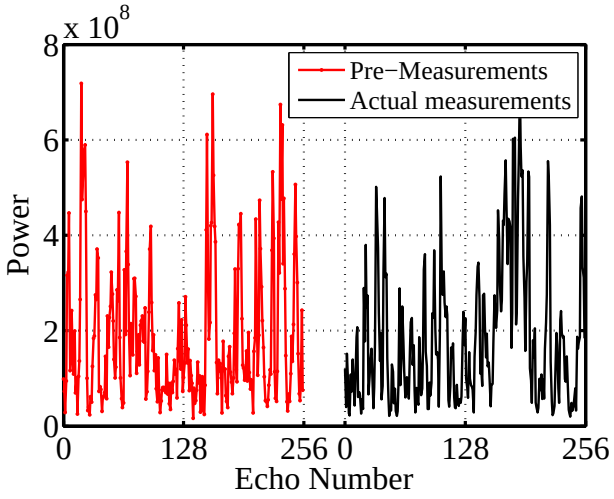

Fig. 4. The power of primary sensor for the pre- and actual measurements, as a function of the echo number.

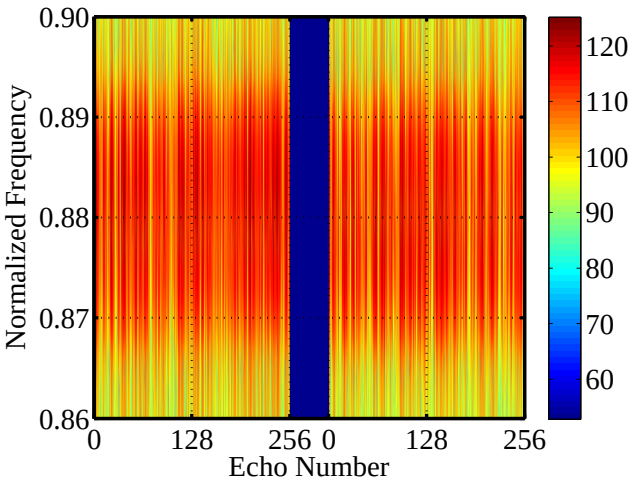

Fig. 5. Spectrogram of the pre- and actual measurements for the primary sensor, as a function of the echo number.

tation of receiver operating characteristic (ROC) curves.

Figures 2 and 3 show the ROC curves for the proposed RFI cancellation algorithm, here termed the dual-channel EPIC (DEPIC) approach, when used in combination with the ETAML detection algorithm presented in [14], for the case of simulated and measured data, respectively. As can be seen from the figures, the proposed RFI cancellation scheme is clearly able to improve the performance as compared to when only the ETAML detector is used. As a comparison, we show the performance of the EPIC algorithm presented in [21], which iteratively subtracts the interference occurring in both the pre- and actual measurements of the primary channel. This method, which in [21] was shown to offer preferable performance as compared to several other cancellation schemes, is designed to use secondary data measured from the same sensor, assuming the RFI to be reasonably stationary over the measurements. As can be seen in Figure 2, EPIC is able to cancel the (fully stationary) RFI component in the simulated data, as may be expected due to the simplistic (and unrealistic) nature of the setup. The DEPIC method is on the other hand unable to cancel the RFI as well as EPIC, due the random difference in amplitude between the two channels, causing a loss in performance. Clearly, if the RFI components can be assumed to be stationary over the pre- and the actual measurements, one should therefore use the secondary data from the same channel to cancel the RFI.

Regrettably, the assumption of stationarity does not seem to hold sufficiently well in a practical setup, and, as can be seen in Figure 3, the RFI cancellation for real measurements using EPIC does not improve the performance of the detector at all as compared to when not using any RFI cancellation. Notably, the performance actually becomes worse than guessing for several false alarm probabilities; this counterintuitive result occurs due the rapidly varying nature of the RFI.

Figure 4 illustrates the power measured over the pre- and actual measurements (here shown as in the left and the right part of the figure, with the gap indicating the delay incurred when changing the setup), as a function of the data block index; as can be seen in the figure, the power of the sensor varies rapidly over time. Similarly, Figure 5 shows the spectrogram of the measured signal, clearly indicating the time varying nature of the RFI. It is worth noting that the desired SOI, which ought to appear as a single common tone in the actual measurement data (the second part of the figure), is completely hidden by the RFI. As a result of time-varying RFI, the spectral subtraction performed by EPIC fails to subtract the appropriate RFI component from the data, and often thereby instead cancels the SOI, or even create an artificial RFI component due to slight phase mismatches in the spectral subtraction, causing the somewhat odd ROC curve.

A similar problem will occur for the existing multi-channel RFI cancellation techniques, such as the methods presented in [12, 22]. These, as well as the methods compared to in those works, are all based on the assumption that the RFI does not vary too rapidly over the echo train, and will therefore suffer from a similar breakdown as EPIC.

5. CONCLUSIONS

In this work, we have introduced a practical dual-channel interference cancellation technique for NQR measurements prone to strong and rapidly time-varying interference signals. The method estimates the interference using the secondary channel and then, compensating for the gain difference between the sensors, subtracts it from the primary channel. The method is in this way able to remove strong interference close to, or at, the NQR frequency. The performance of the method is verified using real measurements of $NaNO_2$.

6. REFERENCES

[1] A. N. Garroway, M. L. Buess, J. B. Miller, B. H. Suits, A. D. Hibbs, A. G. Barrall, R. Matthews, and L. J. Burnett, "Remote Sensing by Nuclear Quadrupole Resonance," *IEEE Trans. Geosci. Remote Sens.*, vol. 39, no. 6, pp. 1108–1118, June 2001.

[2] R. Siegel, "Land Mine Detection," *IEEE Instrum. Meas. Mag.*, pp. 22–28, December 2002.

[3] J. A. S. Smith, M. D. Rowe, R. M. Deas, and M. J. Gaskell, "Nuclear Quadrupole Resonance Detection of Landmines," in *Proc. Int. Conf. Requir. Technol. Detect., Remov. Neutralization Landmines UXO*, H. Sahli, A. M. Bottoms, and J. Cornelis, Eds., Brussels, Belgium, September 15-18 2003, vol. 2, pp. 715–721.

[4] C. Crowley, T. Petrov, O. Mitchell, R. Shelby, L. Ficke, S. Kumar, and P. Prado, "A novel shoe scanner using an open-access quadrupole resonance and metal sensor," in *Proceedings of the SPIE*, 2007, vol. 6538, 65380J.

[5] J. N. Latosinska, "Applications of nuclear quadrupole resonance spectroscopy in drug development," *Expert Opinion on Drug Discovery*, vol. 2, no. 2, pp. 225–248, 2007.

[6] E. Balchin, D. J. Malcolme-Lawes, I. J. F. Poplett, M. D. Rowe, J. A. S. Smith, G. E. S. Pearce, and S. A. C. Wren, "Potential of Nuclear Quadrupole Resonance in Pharmaceutical Analysis," *Anal. Chem.*, vol. 77, pp. 3925–3930, 2005.

[7] T. N. Rudakov, P. A. Hayes, and J. H. Flexman, "Optimised NQR pulse technique for the effective detection of Heroin Base," *Solid State Nuclear Magnetic Resonance*, vol. 33, no. 3, pp. 31–35, 2008.

[8] J. Barras, K. Althoefer, M. D. Rowe, I. J. Poplett, and J. A. S. Smith, "The Emerging Field of Medicines Authentication by Nuclear Quadrupole Resonance Spectroscopy," *Appl. Magn. Reson.*, vol. 43, pp. 511–529, 2012.

[9] G. Kyriakidou, A. Jakobsson, K. Althoefer, and J. Barras, "Batch-Specific Discrimination Using Nuclear Quadrupole Resonance Spectroscopy," *Analytical Chemistry*, 2015.

[10] Y. Tan, S. L. Tantum, and L. M. Collins, "Cramér-Rao Lower Bound for Estimating Quadrupole Resonance Signals in Non-Gaussian Noise," *IEEE Signal Process. Lett.*, vol. 11, no. 5, pp. 490–493, May 2004.

[11] J. Lužnik, J. Pirnat, and Z. Trontelj, "Polarization enhanced 14N NQR detection with a nonhomogeneous magnetic field," *Solid State Communications*, vol. 121, no. 12, pp. 653–656, March 2002.

[12] Y. Jiang, P. Stoica, and J. Li, "Array Signal Processing in the Known Waveform and Steering Vector Case," *IEEE Trans. Signal Process.*, vol. 52, no. 1, pp. 23–35, January 2004.

[13] A. Jakobsson, M. Mossberg, M. Rowe, and J. A. S. Smith, "Exploiting Temperature Dependency in the Detection of NQR Signals," *IEEE Trans. Signal Process.*, vol. 54, no. 5, pp. 1610–1616, May 2006.

[14] S. D. Somasundaram, A. Jakobsson, J. A. S. Smith, and K. Althoefer, "Exploiting Spin Echo Decay in the Detection of Nuclear Quadrupole Resonance Signals," *IEEE Trans. Geosci. Remote Sens.*, vol. 45, no. 4, pp. 925–933, April 2007.

[15] A. Gregorovič and T. Apih, "Improving 14N nuclear quadrupole resonance detection of trinitrotoluene using off-resonance effects," *Solid State Nucl. Magn. Reson.*, vol. 36, pp. 96–98, 2009.

[16] A. Gregorovič and T. Apih, "TNT detection with 14N NQR: Multipulse sequences and matched filter," *J. Magn. Res.*, vol. 198, no. 2, pp. 215–221, June 2009.

[17] N. R. Butt, E. Gudmundson, and A. Jakobsson, "An Overview of NQR Signal Detection Algorithms," in *Magnetic Resonance Detection of Explosives and Illicit Materials*, T. Apih, B. Rameev, G. Mozzhukhin, and J. Barras, Eds., NATO Science for Peace and Security Series B: Physics and Biophysics, pp. 19–33. Springer Netherlands, 2014.

[18] S. D. Somasundaram, A. Jakobsson, M. D. Rowe, J. A. S. Smith, N. R. Butt, and K. Althoefer, "Robust Detection of Stochastic Nuclear Quadrupole Resonance Signals," *IEEE Trans. Signal Process.*, vol. 56, no. 9, pp. 4221–4229, September 2008.

[19] S. D. Somasundaram, A. Jakobsson, and N. R. Butt, "Countering Radio Frequency Interference in Single-Sensor Quadrupole Resonance," *IEEE Geosci. Remote Sens. Lett.*, vol. 6, no. 1, pp. 62–66, Jan. 2009.

[20] A. Svensson and A. Jakobsson, "Adaptive Detection of a Partly Known Signal Corrupted by Strong Interference," *IEEE Signal Process. Lett.*, vol. 18, no. 12, pp. 729–732, Dec. 2011.

[21] J. Swärd and A. Jakobsson, "Interference Cancellation Using Secondary Data," in *22nd European Signal Processing Conference*, Lisbon, Portugal, Sept. 1-5 2014.

[22] N. R. Butt and A. Jakobsson, "Efficient removal of noise and interference in multichannel quadrupole resonance," in *Proceedings of the 45th Asilomar Conference on Signals, Systems and Computers*, nov. 2011, pp. 1072–1076.

[23] G. Kyriakidou, A. Jakobsson, E. Gudmundson, A. Gregorovič, J. Barras, and K. Althoefer, "Improved modeling and bounds for NQR spectroscopy signals," in *22nd European Signal Processing Conference*, Lisbon, Portugal, 2014.

[24] S. D. Somasundaram, *Advanced Signal Processing Algorithms Based on Novel Nuclear Quadrupole Resonance Models for the Detection of Explosives*, Ph.D. thesis, King's College London, London, United Kingdom, 2007.